

# VOLUMETRIC MASS TRANSFER CAPACITY COEFFICIENT IN THE RTL EXTRACTOR

Adil A. Al-Hemiri, Firas Abdul Aziz, and Mu'ayed K. Ibrahim

Chemical Engineering Department – College of Engineering – University of Baghdad – Iraq

## ABSTRACT

The aim of this research work was to determine the overall mass transfer capacity coefficient in the (RTL) Graesser contactor, employing two liquid-liquid systems, viz.:

- I. Kerosene - acetone-water.
- II. Kerosene - MEK-water.

A 0.1 m diameter (RTL) contactor was used for this research work.

Overall mass transfer capacity coefficient ( $K_X.a$ ), which is a product of the specific interfacial area ( $a$ ) and overall mass transfer coefficient ( $K_X$ ), is easier to measure than the individual mass transfer coefficient and specific interfacial area

The results showed that the overall mass transfer capacity coefficient ( $K_X.a$ ), decreased with increasing flow rate of the organic kerosene phase and increased with increasing flow rate of the aqueous phase. Increasing the rotor speed causes increasing in the overall mass transfer capacity coefficient to a maximum value at (30 rpm) and then decreased.

An empirical correlation was found for ( $K_X.a$ ), expressed as a function of operating conditions and back mixing coefficient (Mu'ayed 2001).

$$K_{X.a} = 3.21 \cdot 10^{-4} \cdot \left(\frac{U_C}{U_d}\right)^{0.228} \cdot \left(\frac{N \cdot D_r}{U_d}\right)^{(-0.01)} \cdot \left(1 - \frac{E_B}{U_d \cdot L}\right)^{1.5}$$

## INTRODUCTION

One of the difficulties in designing mass transfer units is obtaining the correct value of the overall mass transfer coefficient ( $K$ ), since this depends on the individual mass transfer coefficients for the dispersed and continuous phase ( $k_d$ ) and ( $k_c$ ). And these coefficients are represented by many equations, some are based on different theories while others were obtained experimentally and each seems to have very limited applications (AL-Hemiri and Kadhim, 2001). This makes the choice of the correct combination of such equations to obtain ( $k_d$ ) and ( $k_c$ ) very difficult.

Another difficulty is the finding of interfacial area ( $A$ ) or the specific interfacial area ( $a$ ) which in turn depends upon the average drop or bubble

size ( $d_{32}$ ). Again there are many relations presented in the literature for the calculation of ( $d_{32}$ ). Most of these relations are based on experimentation on the various mass transfer equipment, using techniques, such as, photography, chemical methods and ultrasonic waves, where none are really reliable.

Thus, this study was initiated to overcome the above mentioned difficulties by determining the capacity coefficient which is the product of the overall coefficient and the specific interfacial area, i.e. ( $K_X.a$ ), rather than the individual coefficients ( $k_c$ ) and ( $k_d$ ) and the specific interfacial area ( $a$ ).

The reason for choosing this contactor is that the specific interfacial area ( $a$ ) of this contactor was reported to be 80-150  $m^2/m^3$  by Alper

(1988, 1989) and to be 42-60 m<sup>2</sup>/m<sup>3</sup> by Al-Hemiri (1995) using chemical methods i.e. extraction with chemical reaction. While in another study using physical method (photography) a value of 60-180 m<sup>2</sup>/m<sup>3</sup> was given (Al-Hemiri and Kareem, 1990). Also, the aqueous phase mass transfer coefficient (KC) was reported to be 2-5x 10<sup>-5</sup> m/s by Alper (1988) and to be 1.5-11.6 x 10<sup>-5</sup> m/s by Al-Hemiri (1995). Although the values of (KC) and (a) reported above are different, however the value of the overall mass transfer capacity coefficient (KC.a) in the two studies were of the same order of magnitude. Thus the capacity coefficient may be a better design criterion than the individual coefficients and the specific surface area.

## EXPERIMENTAL WORK

### Liquid-Liquid Systems

The physical properties of liquid-liquid systems employed are summarized in table (1). This selection is based in general on the availability, low toxicity and difference in physical properties.

Two systems were used, viz., Kerosene-Acetone-Water and Kerosene- MEK-Water.

### Description of Equipment

A 0.1m diameter, 1m long Graesser raining bucket contactor supplied by corning Ltd, was employed. The contactor consist of a horizontal cylindrical shell with a compartment rotor which is made up of a number of circular plates which have "C-shape" buckets mounted near the outer edge between each pair of plates as shown in figure (1).

The contactor is capable of handling a total phase throughput of 12 l/hr at rotor speed of 50 rpm and it consist of 36 compartments, each of 0.025 m long and consists of 6 buckets, each bucket is 0.025 m in diameter and the buckets arrangement is shown in figure (2).

The two phases flow counter-currently along the shell from compartment to another through a peripheral gap between the rotor and the shell. A

short disengaging zone is provided at each end of the unit to ensure complete separation of the phase. The heavy phase, which was aqueous phase, enter and leave the contactor at points just below the rotor shaft, while the light (organic) phase enter and leave at points above the rotor shaft. A 1/3 hp AC motor drives the rotor shaft. The drive shaft of the motor was coupled to the contactor shaft via a gearbox to select the required rpm (0-50 rpm).

Six 0.01 m<sup>3</sup> QVF glass spherical vessels were used as storage reservoirs and were mounted on a special vessel support. Two Stuart-Turner centrifugal pumps, type No. 1 capable of handling 720-750 gphr against 10-45 ft head of water were used to transfer the liquids.

The pumps were made stainless steel and the pump glands were especially adapted for use with solvents.

Flow rates were measured by independently calibrated rotameters. The range of flow of each rotameter is 0-0.01 m<sup>3</sup>/hr of water at 20 oC.

A flow diagram of equipment is shown in figure (3)

### Measurement of Solute Concentration

Concentrations of solute in organic phase and aqueous phase were measured by ultraviolet spectrometry (Robert, et al., 1967).

The instrument for measurement was UV-visible spectrophotometer (Schimadzu 260).

### Experimental Procedure:

The procedure followed during these runs was as follows: first, the dispersed phase solution was made up to the required concentration. After which the contactor was filled with the continuous phase. Then the dispersed phase was introduced into the contactor. Flow rates were adjusted to the required value until the dispersed phase made up to 50% hold-up. The continuous phase flow and the agitator were adjusted to the required values.

After steady state was reached, samples were withdrawn and analyzed using the spectrophotometer, samples taken from the sampling ports at the respective phase outlet at intervals of 15 minutes.

Table (1) Physical properties of systems used

| System                   | Temp. °C | Density Kg/M <sup>3</sup> |       | Viscosity N.s/M <sup>2</sup> *10 <sup>3</sup> |       | Diffusivity M <sup>2</sup> /s*10 <sup>5</sup> |       | Interfacial Tension N/M*10 <sup>3</sup> | Distribution coefficient |
|--------------------------|----------|---------------------------|-------|---|-------|---|-------|---|--------------------------|
|                          |          | Disp.                     | Cont. | Disp.   | Cont. | Disp.   | Cont. |   |                          |
| Kerosene (Acetone) water | 21       | 795.4                     | 998.8 | 1.123   | 1.05  | 2.272   | 1.076 | 39.8                                    | 0.95                     |
| kerosene (MEK) Water     | 24       | 761.7                     | 996.2 | 0.83  | 0.94  | 2.656   | 1.142 | 38.9                                    | 0.64                     |

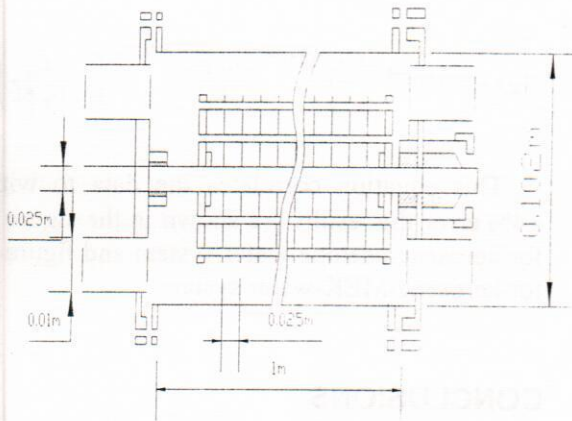


Fig. (1) Schematic diagram of the Graesser contactor buckets (A) longitudinal section of the contactor (B) Cross section of the contactor

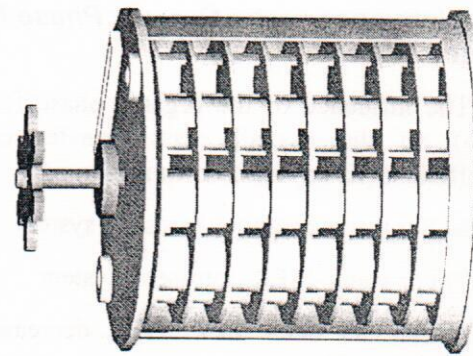


Fig. (2) Schematic diagram shown the buckets arrangement in the Graesser contactor

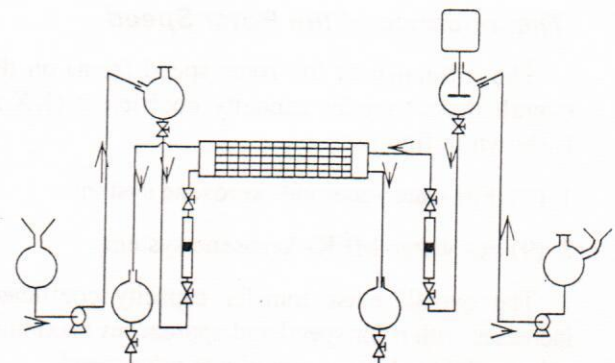


Fig. (3) Schematic flow diagram of the Graesser contactor

## RESULTS AND DISCUSSION

### Influence of Aqueous Phase Flow Rate

The influence of aqueous phase flow rate on the overall mass transfer capacity coefficient ( $K_{X,a}$ ) has shown in figures:

1. (4) For water-acetone- kerosene system
2. (5) For water-MEK- kerosene system

The overall mass transfer capacity coefficient ( $K_{X,a}$ ) increased with increasing aqueous phase flow rate. This may be attributed to the increasing in turbulence of mixing (Wang et al., 1977), however ( $K_{X,a}$ ) for the system kerosene-acetone-water was higher than that for kerosene-MEK-water. This may be due to higher distribution coefficient for the system kerosene-acetone-water than that kerosene-MEK-water system, at the conditions of experiments.

### The Influence of the Organic Phase Flow Rate

The influence of the organic phase flow rate ( $Q_o$ ) on the overall mass transfer capacity coefficient ( $K_{X,a}$ ) has shown in figures:

1. (6) For water-acetone- kerosene system
2. (7) For water-MEK- kerosene system

It can be seen that  $K_{X,a}$  decrease with increasing with increasing organic phase flow rate. This is due to decrease in the concentration of solute on the aqueous side, resulting in higher value of  $\Delta C_{lm}$ .

### The Influence of the Rotor Speed

The influence of the rotor speed (rpm) on the overall mass transfer capacity coefficient ( $K_{X,a}$ ) is shown in figures:

1. (8) For water-acetone- kerosene system
2. (9) For water-MEK- kerosene system

The overall mass transfer capacity coefficient increases with rotor speed and approaches maximum value and then decreases at higher rotor speed.

This effect caused by higher rate of droplets break-up and hence higher interfacial area in the limited range of rotor speed, while further increasing in rotor speed may cause emulsification.

### Mathematical Analysis:

The effect of the operating conditions and back mixing coefficient (Ibrahim 2001) on the overall mass transfer capacity coefficient were correlated in the form of:

$$K_{X,a} = F(UC, U_d, N, Dr, EB, L)$$

Where the notation are given in the list of the symbols.

The resulting dimensioned expression then has the form:

$$K_{X,a} = A_o \cdot \left(\frac{U_C}{U_d}\right)^{A_1} \cdot \left(\frac{N \cdot D_r}{U_d}\right)^{A_2} \cdot \left(1 - \frac{E_B}{U_d \cdot L}\right)^{A_3}$$

Using STATISTICA program, the constant  $A_o$  and the powers were found to be:  $A_o = 3.21 \cdot 10^{-4}$ ,  $A_1 = 0.228$ ,  $A_2 = -0.01$ ,  $A_3 = 1.5$ . Thus the equation obtained has the form:

$$K_{X,a} = 3.21 \cdot 10^{-4} \cdot \left(\frac{U_C}{U_d}\right)^{0.228} \cdot \left(\frac{N \cdot D_r}{U_d}\right)^{-0.01} \cdot \left(1 - \frac{E_B}{U_d \cdot L}\right)^{1.5}$$

This equation correlates the data to with in  $\pm 4\%$  error the results are shown in the figure (10) for kerosene-acetone-water system and figure (11) for kerosene-MEK-water system.

## CONCLUSIONS

From the present study these conclusions were made:

1. Mass transfer capacity coefficient ( $K_{X,a}$ ) decreased with increasing kerosene (light phase) flow rate
2. Mass transfer capacity coefficient ( $K_{X,a}$ ) increased with increasing water flow rate.
3. Increasing rotor speed increased the mass transfer capacity coefficient to a maximum value at rpm (30), then decreased, thus suggesting the best value of rpm.
4. Values of mass transfer capacity coefficients obtained varied from  $(2.49 \cdot 10^{-4} - 3.6 \cdot 10^{-4} \text{ s}^{-1})$  for water-acetone-kerosene system and varied from  $(2.36 \cdot 10^{-4} - 3.42 \cdot 10^{-4} \text{ s}^{-1})$  for water-MEK-kerosene system.
5. An empirical equation was given for  $K_{X,a}$  expressed as a function of operating conditions and back mixing coefficient, with a correlation coefficient of 96 %.

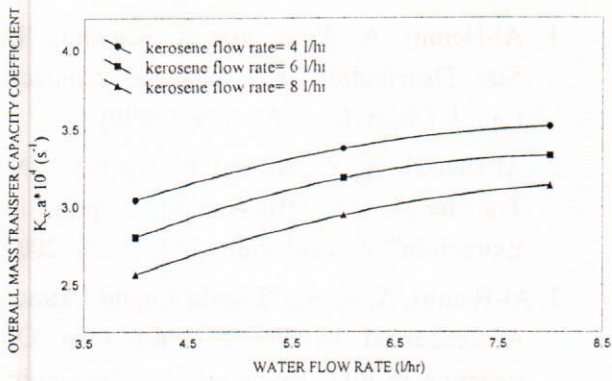


Fig. (4) Effect of water flow rate on overall mass transfer capacity coefficient of kerosene-acetone-water system with different kerosene flow rate and constant rotor speed (10 rpm)

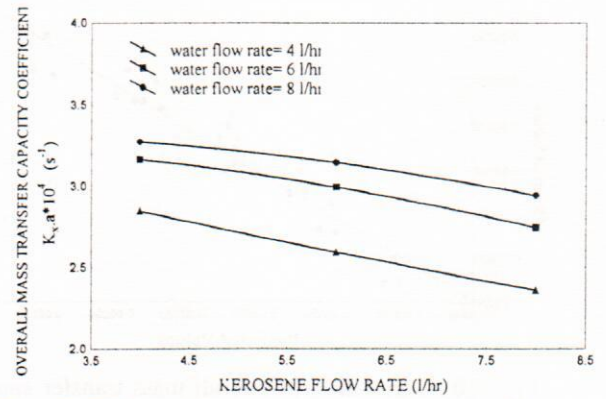


Fig. (7) Effect of kerosene flow rate on overall mass transfer capacity coefficient of kerosene-MEK-water system with different water flow rate and constant rotor speed (10 rpm)

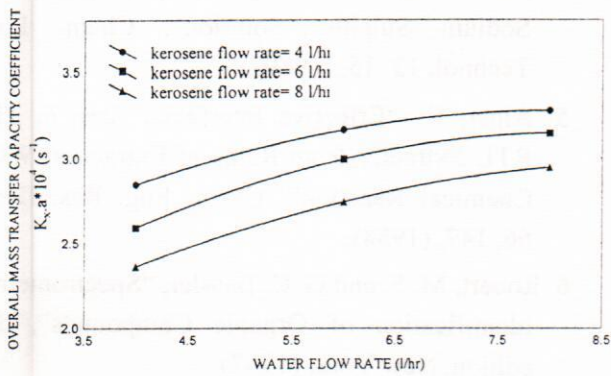


Fig. (5) Effect of water flow rate on overall mass transfer capacity coefficient of kerosene-MEK-water system with different kerosene flow rate and constant rotor speed (10 rpm)

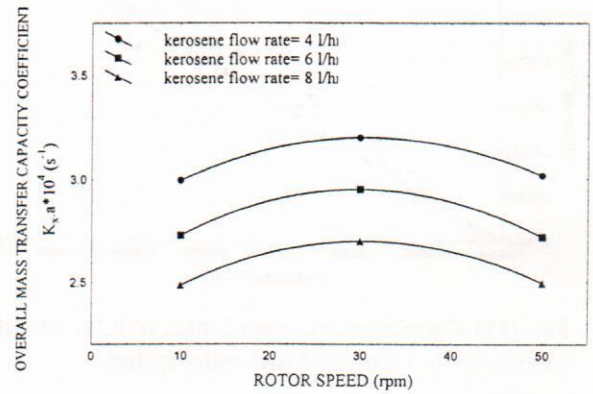


Fig. (8) Effect of rotor speed on overall mass transfer capacity coefficient of kerosene-acetone-water system with different kerosene flow rate and constant water flow rate (4 l/hr)

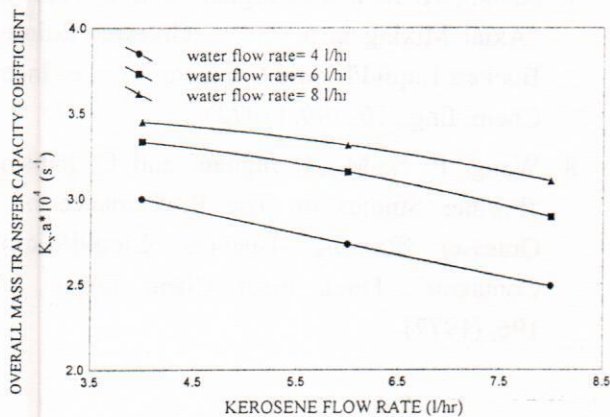


Fig. (6) Effect of kerosene flow rate on overall mass transfer capacity coefficient of kerosene-acetone-water system with different water flow rate and constant rotor speed (10 rpm)

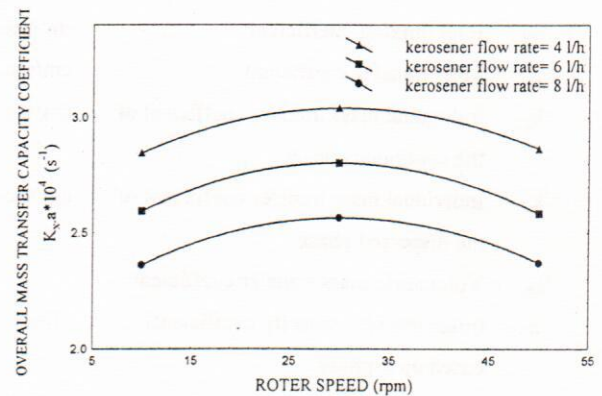


Fig. (9) Effect of rotor speed on overall mass transfer capacity coefficient of kerosene-MEK-water system with different kerosene flow rate and constant water flow rate (4 l/hr)

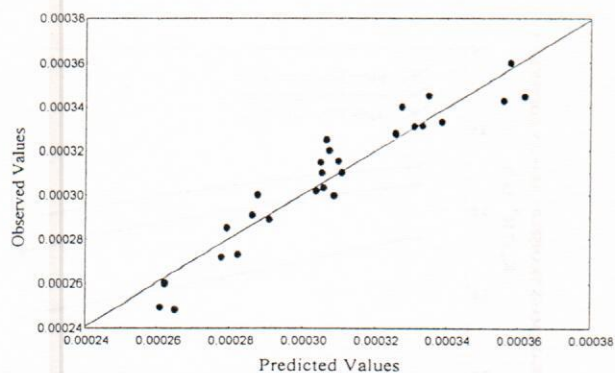


Fig. (10) Correlation of overall mass transfer capacity coefficient for kerosene-acetone-water system

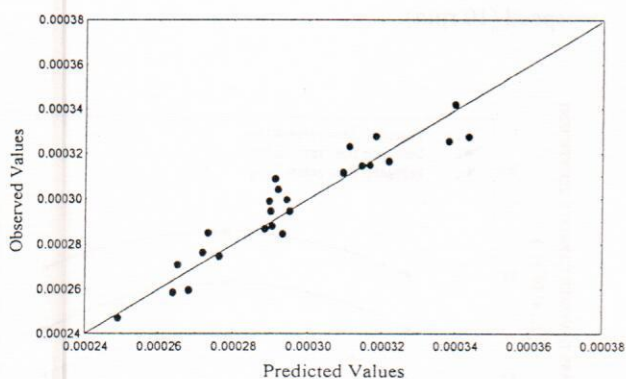


Fig. (11) Correlation of overall mass transfer capacity coefficient for kerosene-MEK-water system

### SYMBOLS

|                |  |                                  |
|----------------|--|----------------------------------|
| A              | Interfacial mass transfer area   | cm <sup>2</sup>                  |
| a              | Specific interfacial mass transfer area  | cm <sup>2</sup> /cm <sup>3</sup> |
| D <sub>r</sub> | Disk diameter  | Cm                               |
| E <sub>B</sub> | Back-mixing coefficient  | cm <sup>2</sup> /sec.            |
| K              | Mass transfer coefficient  | cm/sec.                          |
| k <sub>c</sub> | Individual mass transfer coefficient of the continuous phase                               | cm/sec.                          |
| k <sub>d</sub> | Individual mass transfer coefficient of the dispersed phase                                | cm/sec.                          |
| K <sub>x</sub> | Volumetric mass transfer coefficient (mass transfer capacity coefficient) based on x-phase | 1/sec.                           |
| L              | Length of contactor  | m                                |
| U <sub>c</sub> | Superficial velocity of continuous phase   | cm/sec.                          |
| U <sub>d</sub> | Superficial velocity of dispersed phase  | cm/sec.                          |

### REFERENCES

1. Al-Hemiri, A. A. A. and A. Kaream, "Drop Size Distribution in a Graesser Contactor", *Can. J. Chem. Eng.*, 68, 569, (1990).
2. Al-Hemiri, A. A. A. and R. Kadhim, "Mass Transfer Coefficient in Liquid-Liquid Extraction", *Al-Muhandis*, 145, 1, 75, (2001)
3. Al-Hemiri, A. A. A., "Liquid-Liquid Extraction Accompanied by Pseudo Fast First Order Reaction in RTL Extractor", *Al-Muhandis*, 1, 121, 14, (1995).
4. Alper, E. and Basel Abu-Sharkh "Performance of an RTL Contactor for Gas-Liquid System: Effective Interfacial Area and Volumetric Mass Transfer Coefficient By Oxidation of Sodium Sulphite Solution", *Chem. Eng. Technol.* 12, 15, (1989).
5. Alper, E., "Effective Interfacial Area in The RTL Extractor from Rates of Extraction With Chemical Reaction", *Chem. Eng. Res. Des.*, 66, 147, (1988).
6. Robert, M. S. and G. C. Bassler, "Spectrometric Identification of Organic Compounds", 2<sup>nd</sup> edition, New York, (1967).
7. Mu'ayed, K. I., " Volumetric Mass Transfer Capacity Coefficient Back Mixing Coefficient in the RTL Extractor", 2001, M.Sc. Thesis, Baghdad University.
7. Sheikh, A. R. and J. Ingham and C. Hanson, "Axial Mixing in a Graesser Raining Buckets Liquid/Liquid Contactor" *Trans. Instn. Chem. Eng.*, 50, 199, (1972).
8. Wang, P. S. M., J. Ingham and C. hanson, "Further Studies on The Performance of a Graesser Raining Buckets Liquid/Liquid Contactor", *Trans. Instn. Chem. Engrs.*, 55, 196, (1977).